neuroglia

MDPI

Article

Ultrastructural Remodeling of the Neurovascular Unit in the Female Diabetic db/db Model–Part II: Microglia and Mitochondria

Melvin R. Hayden [1,2,*], DeAna G Grant [3], Annayya R. Aroor [1,2,4] and Vincent G. DeMarco [1,2,4,5]

1 Diabetes and Cardiovascular Center, University of Missouri School of Medicine, Columbia, MO 65212, USA; aroora@health.missouri.edu (A.R.A.); demarcov@missouri.edu (V.G.D.)
2 Division of Endocrinology and Metabolism, Department of Medicine, University of Missouri, Columbia, MO 65211, USA
3 Electron Microscopy Core Facility, University of Missouri, Columbia, MO 65211, USA; GrantDe@missouri.edu
4 Research Service, Harry S. Truman Memorial Veterans Hospital, Columbia, MO 65291, USA
5 Department of Medical Pharmacology and Physiology, University of Missouri, Columbia, MO 65211, USA
* Correspondence: mrh29pete@gmail.com; Tel.: +1-573-346-3019

Received: 27 August 2018; Accepted: 27 September 2018; Published: 7 October 2018

Abstract: Obesity, insulin resistance, and type 2 diabetes mellitus are associated with diabetic cognopathy. This study tested the hypothesis that neurovascular unit(s) (NVU) within cerebral cortical gray matter regions may depict abnormal cellular remodeling. The monogenic (*Lepr^{db}*) female diabetic db/db [BKS.C*Dock7^{m}* +/+*Lepr^{db}*/J] (DBC) mouse model was utilized for this ultrastructural study. Upon sacrifice (20 weeks), left-brain hemispheres of the DBC and age-matched nondiabetic control C57BL/KsJ (CKC) mice were immediately immersion-fixed. We observed an attenuation/loss of endothelial blood–brain barrier tight/adherens junctions and pericytes, thickened basement membranes, adherent red and white blood cells, neurovascular unit microbleeds and pathologic remodeling of protoplasmic astrocytes. In this second of a three-part series, we focus on the observational ultrastructural remodeling of microglia and mitochondria in relation to the NVU in leptin receptor deficient DBC models. This study identified novel ultrastructural core signature remodeling changes, which consisted of invasive activated microglia, microglial aberrant mitochondria with nuclear chromatin condensation and adhesion of white blood cells to an activated endothelium of the NVU. In conclusion, the results implicate activated microglia in NVU uncoupling and the resulting ischemic neuronal and synaptic damage, which may be related to impaired cognition and diabetic cognopathy.

Keywords: astrocyte; db/db mouse model; microglia; mitochondria; neuroglia; neurovascular unit; type 2 diabetes

1. Introduction

Previously, we have overviewed the background, and documented the observations of the 20-week old female db/db [BKS.C*Dock7^{m}* +/+*Lepr^{db}*/J] (DBC) and its comparison to the age-matched control (CKC) model with a focus on ultrastructure protoplasmic astrocyte remodeling in relation to the neurovascular unit (NVU) [1]. We demonstrated marked multicellular ultrastructure remodeling comprised by the following: (i) attenuation and/or loss of blood–brain barrier tight and adherens junctions (TJ/AJ); (iia) adherent red blood cells to endothelial cell(s) (EC) of the NVU; (iib) microbleeds of the NVU; (iic) endothelial cell thinning and activation with white blood cell adherence to

ECs; (iii) maladaptive pericyte attenuation and/or loss; (iv) NVU basement membrane thickening; (v) detachment and retraction of protoplasmic astrocytes from the NUV [1]. In this second of a three-part series our focus will be on the microglia, mitochondria and white blood cell adhesion to the neurovascular unit endothelial cell in the diabetic DBC as compared to the nondiabetic control CKC models. The identifying ultrastructure characteristics of microglia have been described in our previous article [1] and are illustrated (Figure 1). Additional supplemental videos are also provided.

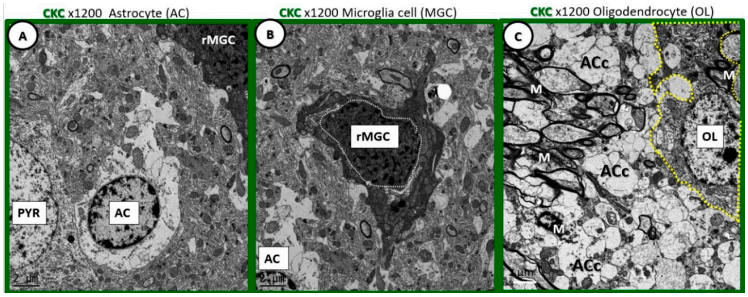

Figure 1. Comparison of ramified microglia to glia and pyramidal cells in cortical grey matter layer III to supplement the extracted description from Table 1 [1]. (**A**) Depicts an astrocyte (AC) with electron lucent cytoplasm with a neuronal pyramidal (PYR) cell immediately adjacent. (**B**) Depicts a ramified microglial cell (rMGC) with its highly electron-dense cytoplasm and nucleus outlined by white dashed line. (**C**) Depicts just a partial image of an oligodendrocyte (OL) in the transition zone between the cortical grey matter and white matter. Note the ramified cytoplasmic extensions. Microglia are the smallest of the glia cells and their cytoplasm is the most electron-dense of the neurovascular unit (NVU) cells and brain cortical grey matter. In their nonactivated phenotypic state, they have elongated cytoplasmic process in ramified form. They have an extensive endoplasmic reticulum, Golgi body system and contain multiple mitochondria. Their cytoplasmic processes are known to be capable of extending and contracting. They have a unique morphology of their nuclei with an outer stippled chromatin at its neurolemma and a more stippled diffuse chromatin electron-dense appearance of the central nuclei. Magnification 1200×; bar = 2 μm.

Microglial cells are the resident innate immune cells of the brain, which represent approximately 5–20% of the brain neuroglial population and have a large number of membranous and intracellular microglial markers; a large number of signaling molecules, which include numerous microglial cytokines and chemokines [2]. Microglia contribute to the regulation of brain development, shaping synaptic connectivity within neuronal networks and are of major importance in brain defense injury [2–4]. In the healthy brain, ramified microglia are constantly surveilling their regional environment and provide the necessary housekeeping-cleaning-gatekeeping functions to maintain brain tissue homeostasis (Figure S1, Figure S2 and Video S1). Microglia are capable of producing numerous free radicals (superoxide, reduced nicotinamide adenine dinucleotide phosphate (NADPH Ox), inducible nitric oxide and mitochondrial-derived reactive oxygen/nitrogen (mtROS)) and are the major killing and phagocytic cell in the brain if bacterial, viral or parasitic infections become invasive. Importantly, microglia are able to return to return to their surveilling-ramified phenotype once the invaders or danger–damage signals have been eradicated and assume their normal cellular debris housekeeping role [2–12].

Mesoderm (yolk sac)-derived microglia cells are the first and main form of active immune defense in the brain [2–12]. Microglia are unique from bone marrow derived peripheral monocyte-macrophage cells in that they are not dependent on recruitment from the peripheral systemic circulation but are capable of undergoing proliferation mechanisms if needed [13]. Microglia may play both a protective role of surveillance for injury to the NVU unit (Figure S2, Figure S3 and Video S2) as well as a possible damaging role to the NVU in the DBC models due to microglia invasiveness with resulting detachment and separation of protoplasmic astrocytes from the BM of the endothelial cells and pericytes of the NVU [1].

We originally hypothesized that microglia might demonstrate some of their reactive changes similar to our previous observations in the diet-induced obesity and insulin resistant Western models with impaired intermittent glucose elevation [14].

Microglia in CKC animals display distinct phenotypes in transmission electron microscopy (TEM) (Joel 1400-EX TEM JOEL (JOEL, Peabody, MA, USA) images and these cells will be referred to as ramified microglial cells (rMGC). These cells survey their surrounding milieu of endothelial cells, pericytes, astrocytes of the NVU and neurons. They maintain this ramified phenotype and function in association with intact tight and adherence junctions of the ECs blood–brain barrier and the intact adherent protoplasmic astrocytes to the basement membrane of the NVU. Ramified microglia cells are constantly prepared to undergo a rapid diverse phenotypic remodeling change to what we will reference as the activated-amoeboid microglial cell phenotype (aMGC). These changes may be due to morphological remodeling and/or the expressions of their cell surface receptors in response to danger or damage signals such as pathogen associated molecular patterns (PAMPs) or damage associated molecular patterns (DAMPS) due to oxidized/glycated proteins/polypeptides, lipids, and nucleic acids from their diabetic hyperglycemic microenvironment [2–13]. The phenotypic remodeling changes need to be qualified by the model (i.e., control CKC or diabetic DBC), the region of the brain (as in our gray matter cortical layer III), the disease state (obesity, insulin resistance and type 2 diabetes mellitus (T2DM)) and their age (20 weeks) [2–13]. Activated microglial phenotypes have been classified by some to be similar to peripheral macrophages, i.e., M1 (classically activated macrophages) and M2 (alternatively activated macrophages) cells [7,8]; however, the possibly more preferred method of identification of MGCs relies on individual cell surface markers or their response to inducible cytokines [9–11]. We have chosen to utilize only rMGC or aMGC when referring to our morphofunctional–pathomorphologic phenotypic polarization in TEM observations (Figure 2).

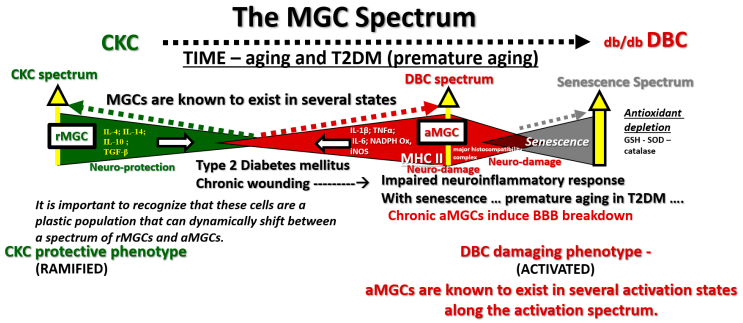

Figure 2. Microglia spectrum phenotypes in type 2 diabetes mellitus (T2DM). The microglia cell(s) (MGC) are very unique and capable of undergoing a marked diversity of morphological and functional phenotypic remodeling change as they pass along a spectrum of phenotypes from the ramified MGC (rMGC) (green colorization) on the far left-hand side of this cartoon to the chronically activated-amoeboid microglia cells (aMGC) (red colorization) on the right hand in addition to some microglia progressing to a senescent type of MGC on the far right (grey colorization), which may implicate advanced aging. Note the various cytokines profiles associated with each of the rMGC and the aMGC phenotypes. In our age-matched nondiabetic control C57BL/KsJ (CKC) models, the predominate MGC would be rMGC and in the DBC models the predominant microglia would be aMGC since we are only studying the ultrastructural phenotypic ultrastructural remodeling changes. Note that in health or homeostasis we demonstrate that the MGC may be in a flux or spectral change between rMGCs and more activated/amoeboid MGCs. The regions between open arrows may even represent a range of homeostasis between rMGCs and versatile aMGCs phenotypes, while the dashed lines suggest multiple spectral morphologic phenotypes. IL-1β: interleukin 1 beta; IL-14: interleukin 14; IL-10: interleukin 10; TGF-β: Transforming growth factor beta; TNFα: tumor necrosis factor alpha; IL-6: interleukin 6; NADPH Ox: reduced nicotinamide adenine dinucleotide phosphate; Inos: inducible nitric oxide synthase; GSH: glutathione; SOD: superoxide dismutase.

2. Materials and Methods

2.1. Sample Preparation for Serial Block Face Imaging: Focused Ion Beam/Scanning Electron Microscopy for Supplemental Video 3

Samples were prepared following a modified version of NCMIR (National Center for Microscopy and Imaging Research) methods for three-dimensional (3D) EM. Unless otherwise stated, all reagents wefre purchased from Electron Microscopy Sciences and all specimen preparation was performed at the Electron Microscopy Core Facility, University of Missouri. Tissues were fixed in 2% paraformaldehyde, 2% glutaraldehyde in 100 mM sodium cacodylate buffer pH = 7.35. Next, fixed tissues were rinsed with 100 mM sodium cacodylate buffer, pH = 7.35 containing 130 mM sucrose. Secondary fixation was performed using equal parts 4% osmium tetroxide and 3% potassium ferrocyanide in cacodylate buffer and incubated on ice for 1 h, then rinsed with cacodylate buffer and further with distilled water. En block staining was performed for one hour in a 1% thiocarbohydrazide solution followed by distilled water rinses. Rinsed tissues were incubated in an additional 2% aqueous osmium tetroxide solution for 30 min at room temperature, then rinsed with distilled water. Additional en bloc staining was performed using 1% aqueous uranyl acetate and incubated at 4 °C overnight, then rinsed with distilled water. A final en bloc staining was performed using Walton's Lead Nitrate solution (Lawrence Livermore Laboratory University of California, Livermore, CA, USA) for 30 min at 60 °C. Tissues were rinsed and dehydrated using ethanol, transitioned into acetone, and then infiltrated with Durcapan resin and polymerized at 60 °C overnight. Block faces were prepared using an ultramicrotome (Ultracut UCT, Leica Microsystems, Germany) and a diamond knife (Diatome, Hatfield, PA, USA) and mounted on an SEM stub and coated with 20 nm of platinum using the EMS 150T-ES Sputter Coater (Leica Microsystems Inc. Buffalo Grove, IL USA). Serial block face data was acquired on a Thermo Fisher Scientific Scios Analytical Dualbeam (Hillsboro, OR, USA). The region of interest was identified using established landmarks and protected with a 1-µm layer of platinum using the ion column. Trenches were rough cut to the side and the front of the block face using a high ion beam current (30 kV 5 nA) to expose the desired block face. Next, the block face was polished using an ion beam current of 50 pA prior to collecting serial images using the Slice &View automated software package. Serial sections were cut at a thickness of 20 nm (30 kV 1 nA) and SEM images were acquired at 2 keV and 25 pA using the T1-BSE detector and reverse contrast. Image segmentation was performed using ThermoScientific Amira 6 Software (Thermo Fisher Scientific). Approximately 250 slices were obtained to create the video for Supplementary Video S3.

2.2. Microglia Ultrastructure Examination and Observation

Three models per group were studied by TEM (n = 3 in control CKC and in diabetic DBC models). Regions of interest were selected based on the presence of NVU capillaries in gray matter cortical layer III. A total of 60 microglia were eventually studied for all models with 10 from each model providing 30 microglia from CKC and 30 from DBC models. Age-matched nondiabetic control C57BL/KsJ microglia demonstrated 28 of 30 with ramified cytoplasmic projections, 5 of 30 microglia with aMt of 5–6 or more and 3 of 30 with some degree of nuclear chromatin condensation, while in DBC 9 of 30 microglia demonstrated ramifications, 25 of 30 microglia demonstrated aberrant Mt (aMt) with 6–14 aMt and 24 of 30 depicted marked chromatin condensation. Herein, we depict representative ultrastructural remodeling changes in aMGC of the diabetic DBC compared to the rMGC in control CKC models.

3. Results

3.1. Microglial Cell of the Neurovascular Unit in Control CKC Model

Microglial cells reside throughout the brain parenchyma and are frequently adjacent to the endothelial cell, pericytes, mural cells and astrocytes of the NVU in the cortical grey matter of layer III.

The normal ultrastructure morphology of ramified microglial cells in control models (CKC) in relation to the NVU and other interstitial regions are depicted (Figures 3 and 4).

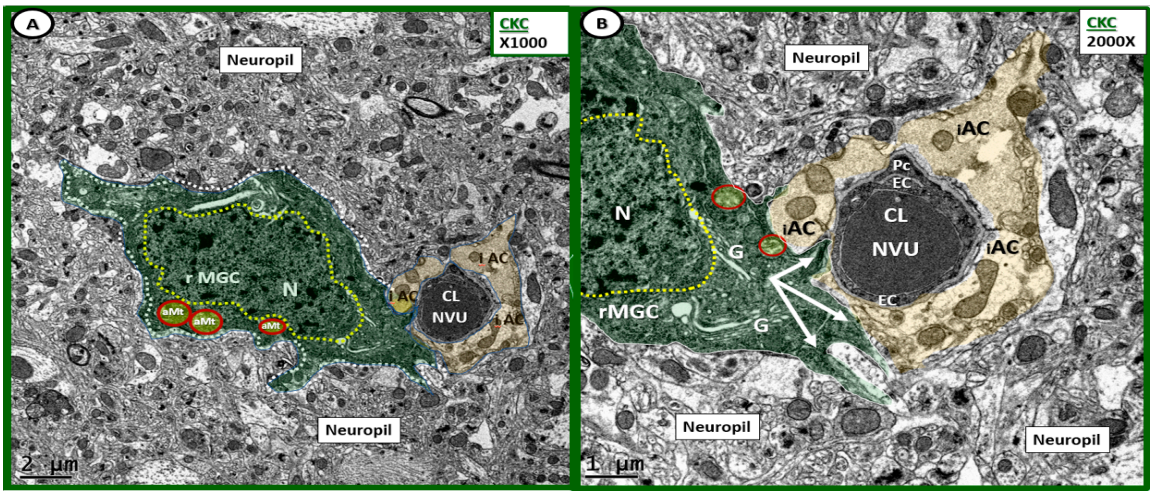

Figure 3. Ramified microglia as a part of the neurovascular unit in control CKC models. (**A**,**B**) Depict the normal ultrastructure of the ramified microglia cells in the control CKC models at different magnifications. (**A**) Depicts a ramified microglia cell (rMGC) phenotype surveilling the NVU. Note how the rMGC cytoplasmic processes (pseudo-colored green) appear to slide in between the intact astrocytes (pseudo-colored golden iAC) in panel (**A**,**B**) as if surveilling or probing the NVU (arrows in panel (**B**) for danger or damage signals. Ramified MGCs are known to have a stippled outer chromatin electron density and also a diffuse inner stippled chromatin arrangement. Also, note the aberrant Mt (aMt) numbering 3 in panel (**A**) and two in panel (**B**) (pseudo-colored yellow with red outline), which are in contrast to the multiple aMt in the DBC depicted later. (**A**) Magnification ×1000; scale bar = 2 µm; (**B**) Magnification ×2000; scale bar = 1 µm. Cl: capillary lumen; EC: endothelial cell; G: Golgi body; iAC: intact astrocyte; N: nucleus: Pc: pericyte.

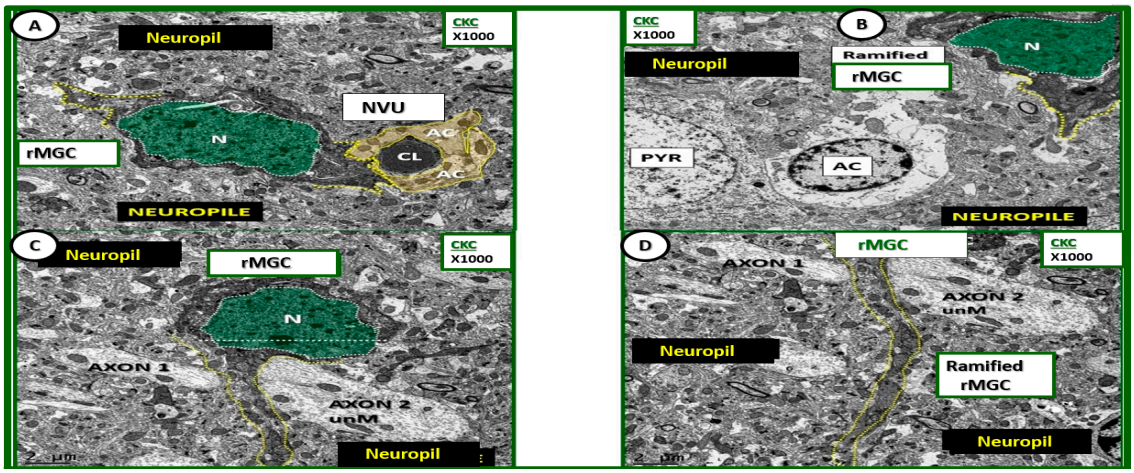

Figure 4. Ultrastructure of ramified microglia in control CKC models. (**A**–**D**) Depict the normal ultrastructure of the ramified microglia (rMGC) in nondiabetic control CKC models. Ramified microglia typically have elongated cytoplasmic processes (yellow-dashed lines) and they typically have a large prominent nucleus (N) (pseudo-colored green and outlined with white-dashed line). Note the diffuse electron-dense chromatin pattern that will undergo extensive chromatin condensation-clumping in activated microglia of diabetic DBC models depicted later. Magnification ×1000; scale bar = 2 µm. AC: astrocyte; CL: capillary lumen; NVU: neurovascular unit; PYR: pyramidal cell.

We have previously demonstrated how the ramified microglia with their elongated processes are very responsive and mobile in cleaning Layer III of the cortical grey matter in the diet-induced Western models (Figure S1, Figure S2 and Video S1). Interestingly, the more proximal somal regions of microglia appear linearly and are observed to be attached to one another similar to box cars of a train between layer III and layer IV and thus, we refer to them as 'trains of microglia' (Video S2). We also observed microglia interrogating the NVU; however, in Western models they appear to back away and do not invade the NVU (as in diabetic DBC models discussed later) since they do not detect any danger or damage signals and do not invade the NVU and appear to back away from the NVU (Video S2).

3.2. Microglia Remodeling in Diabetic DBC Models

The aMGC in DBC models were observed to invade the endothelial cells of the NVU and were associated with the detachment and separation / retraction of the astrocyte from the NVU, attenuation and/or loss of the TJ/AJ in the blood brain barrier (BBB) of the NVU and have aberrant mitochondria and chromatin condensation (Figures 5 and 6)

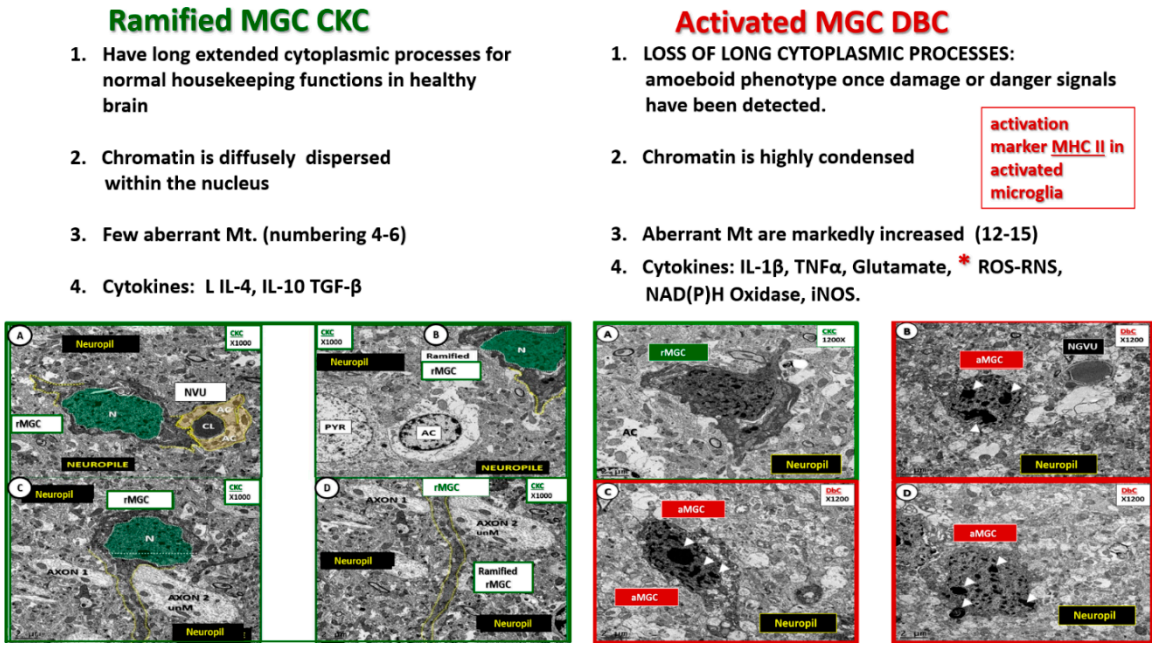

Figure 5. Comparison of ramified MGC to an activated MGC in control CKC and diabetic DBC models. (**A**–**D**) Depict the ramified (rMGC) (colorized with green nucleus) to demonstrate at low magnification the different morphology of the rMGC as compared to the activated aMGC DBC model (**B**–**D**). One notes the aMGC assumes a more amoeboid morphology in the DBC model (**B**–**D**) on the right outlined in red as compared to the CKC models on the left with CKC with ramified cytoplasmic extensions (outlined with yellow dashed lines). Also note that the nuclear chromatin is condensed, aggregated/clumped in the DBC models on right when compared to the diffuse nuclear chromatin in the CKC on the left. Importantly, note the major differences between the CKC and DBC in the upper 1–4 numbered major differences between CKC rMGC and DBC aMGC. The low magnification in these images is unable to demonstrate or appreciate the differences in mitochondria in these images. Magnification ×1000 (**A**–**D** in CKC) and ×1200 (**A**–**D** in DBC); Scale bar = 2 µm.

Microglial cells undergo ultrastructural maladaptive remodeling changes to the cytoplasmic and nuclear components including cytoplasmic aMt that are characterized by markedly swollen mitochondria with loss of electron-dense mitochondrial matrix proteins and crista in the cytoplasm and nuclear chromatin condensation in addition to becoming invasive of the NVU (Figure 7) (Figure S4 and Video S3).

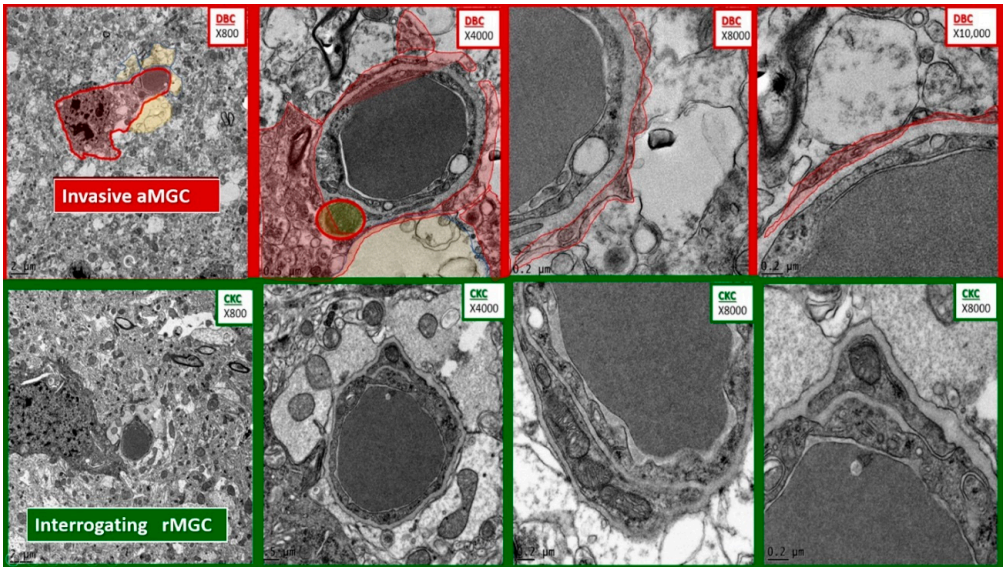

Figure 6. Comparison of microglia invasion in the diabetic DBC and interrogation in control CKC models. The top four panels depict the invasiveness of an activated microglial cell (aMGC) (pseudo-colored red) with marked chromatin clumping–aggregation invading a NUV with capillary lumen in progressively increased magnifications from left to right. Note the thin rim of the aMGC cytoplasmic extensions as it approaches the NVU and begins to encircle the enclosed endothelial and pericyte basement membrane with early detachment of the normally adherent intact astrocyte. In some images they will result in the complete astrocyte detachment and retraction from the NVU. Magnifications at the top right of each image and scale bars are indicated in the lower left of each panel. In the lower four panels of comparable magnifications note how the rMGC is only undergoing an interrogating function and does not invade the NVU.

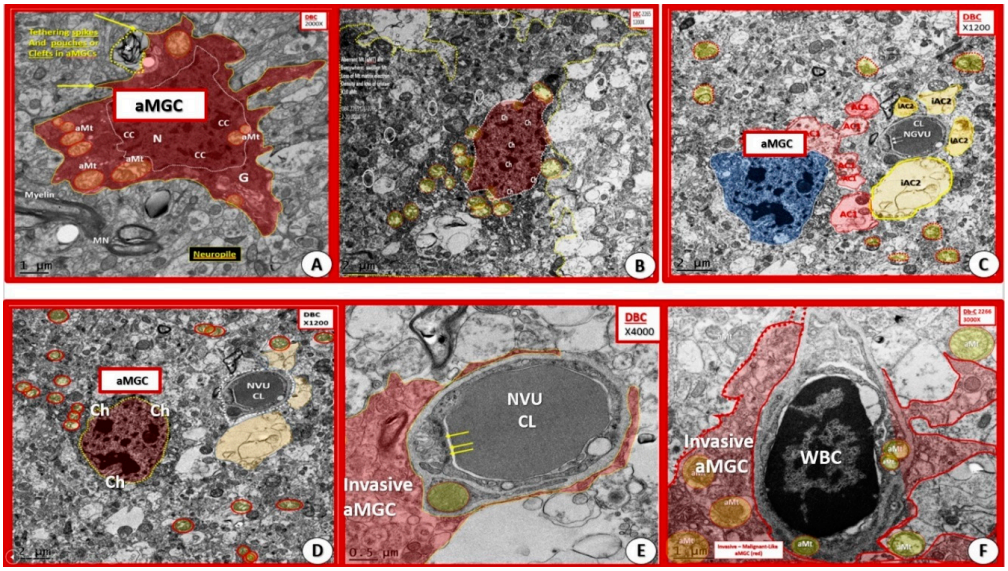

Figure 7. Activated microglia become invasive of the neurovascular unit in diabetic DBC models. Panels (**C**–**F**) depict how activated MGCs (aMGCs) become invasive to the NVU in DBC models. In contrast to the CKC ramified MGC (rMGC), which are surveilling, aMGC (pseudo-colored red except for the 'frown-faced' aMGC (pseudo-colored blue)) nucleus in (**C**). Panel F depicts a mononuclear white blood cell (lymphocyte) (WBC) adherent to the luminal NVU endothelial cell. Magnification ×2000 (**A**); ×1200 (**B**–**D**); ×4000 (**E**); ×3000 (**F**) with varying scale bars lower left of each panel.

Activated-amoeboid microglia have a marked increase in cytoplasmic aMt and also demonstrate extensive nuclear chromatin condensation in contrast to a diffuse stippled chromatin pattern in CKC and contain increased numbers of aberrant mitochondria within the cytoplasm, as compared to the ramified microglia in controls Figures 8–12.

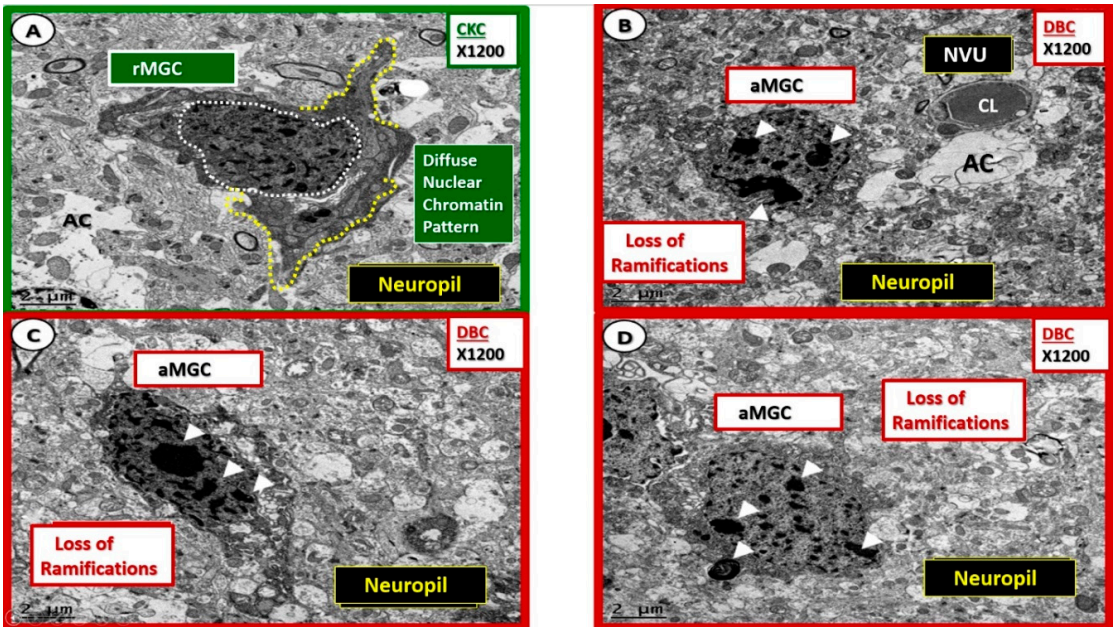

Figure 8. Nuclear chromatin condensation of activated microglia in diabetic DBC models. (**A**) Depicts the appearance of the nucleus with diffuse nuclear chromatin pattern (outlined in white dashed lines) and ramified cytoplasmic extensions (yellow dashed lines). Panels (**B**–**D**) demonstrate a distinct phenotypic nuclear chromatin condensation (arrowheads) within the nuclei of the activated microglia cells (aMGC) in the diabetic DBC as compared to the ramified microglia cells (rMGC) in control nondiabetic CKC models. Specifically, note the unusual 'frown-faced' nuclei in panel **B** due to nuclear chromatin condensation. Magnification ×1200; scale bar = 2 µm. CL: capillary lumen; NVU: neurovascular unit.

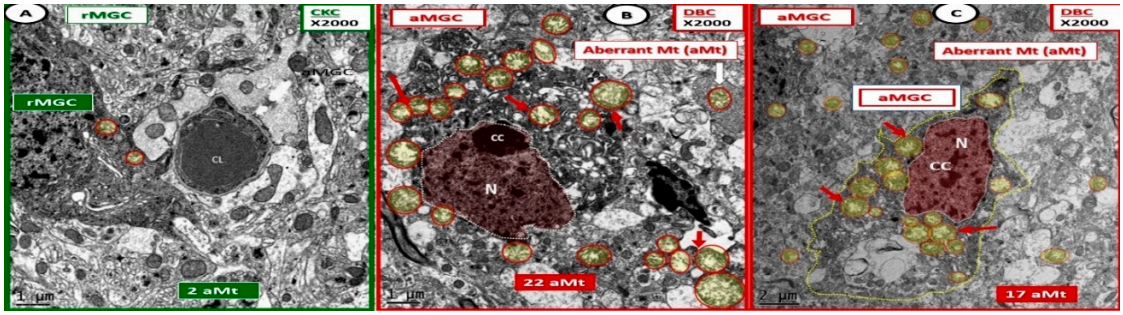

Figure 9. Activated microglia cells depict aberrant mitochondria in diabetic DBC models. Panels (**B,C**) illustrate the pseudo-colored red nuclei of activated microglia cells (aMGC) and the aberrant mitochondria (aMt) (pseudo-colored yellow with encircling red lines) (arrows) that are markedly increased in number and demonstrate marked mitochondrial (Mt) swelling with loss of electron-dense Mt matrix and crista as compared to control CKC model (**Panel A**) in diabetic DBC. Aberrant Mt will also be observed in other neurovascular unit cells and neurons in later images. Also, some aMGCs were extremely dark as in panel (**B**). However, all MGC are dark when compared to other glia and neurons. Magnification ×2000; bar = 1 µm in panels (**A,B**) and bar = 2 µm in panel (**C**). CC: chromatin condensation; CL: capillary lumen; N: nucleus.

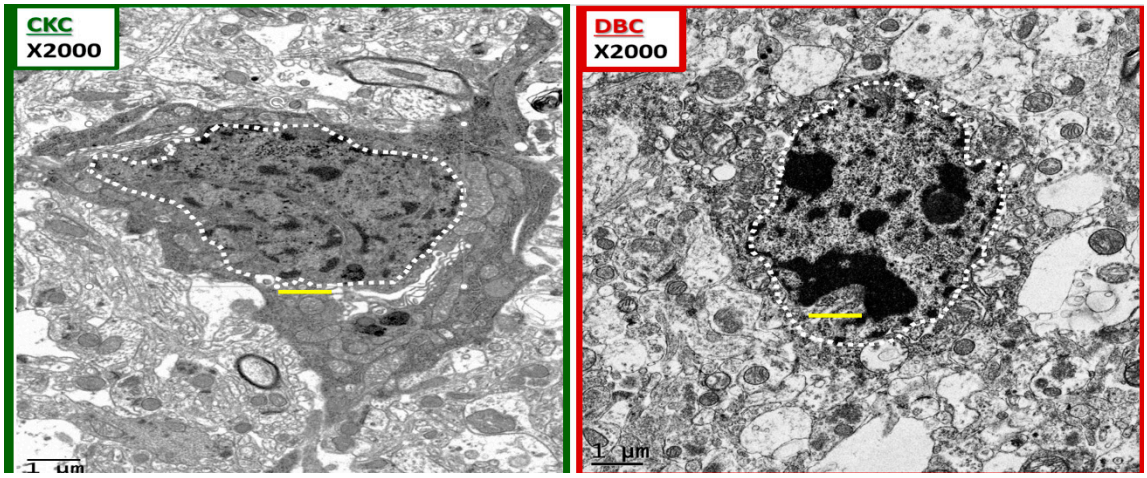

Figure 10. Chromatin condensation in the diabetic DBC. The above images depict ramified and amoeboid-activated microglia in a side-by-side comparison. A ramified microglia (rMGC) on the left with a stippled outer chromatin at the neurolemma and a diffuse stippling of chromatin within the core of the nucleus in the control CKC. In contrast, the amoeboid-activated microglia (aMGC) on the right depicts marked nuclear chromatin condensation in the DBC. Note that in the aMGC of the diabetic DBC the nuclear chromatin condensation–compaction volume is markedly greater than in the nondiabetic control rMGC CKC models. Magnification ×2000; scale bar = 1 µm and was copied and placed within the nuclei to appreciate the sizes of the chromatin.

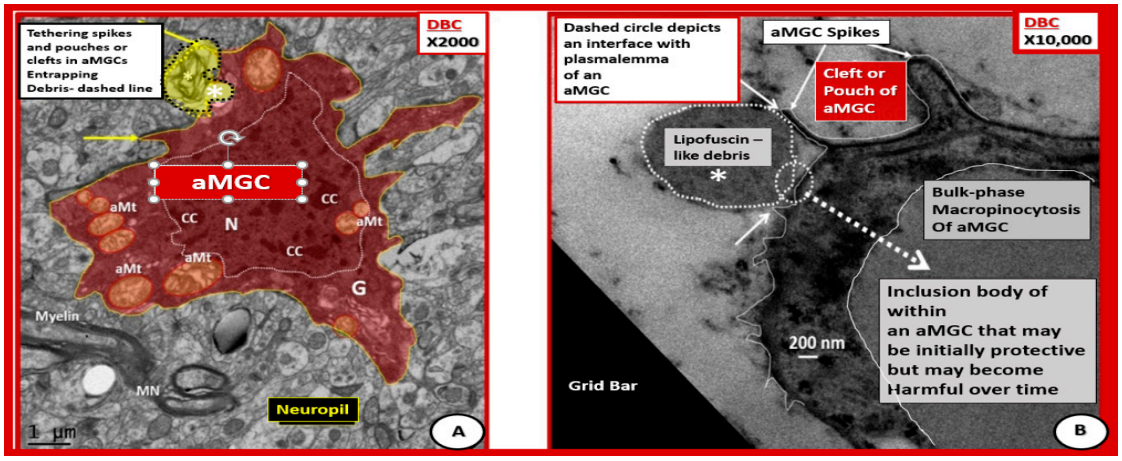

Figure 11. Activated microglia with aberrant mitochondria and tethering spikes and pouches in diabetic DBC. (**A**) Depicts a pseudo-colored red aMGC. (**B**) Depicts a high magnification of a portion of an outer cytoplasmic MGC phagocytosing lipofuscin-like debris. In (**A**), the plasma membrane appears to be taking up a residual body (dashed line with yellow color) and uptake of lipofuscin-like debris (white dashed line) in (**B**). Panel (**A**) depicts spikes (arrows) and pouches or clefts and aberrant mitochondria (aMt) (pseudo-colored yellow with red outer lines). Panel B illustrates bulk phase macropinocytosis of lipofuscin-like debris across the plasma membrane and appears to be being deposited within the cytoplasm of an aMGC. These two aMGCs are different cells but both are within the cerebral cortical grey matter in layer III and demonstrate the important process of phagocytosis. Note the prominent chromatin condensation (CC) within the nucleus. Panel A magnification ×2000; bar = 1µm. Panel B magnification ×10,000; bar = 200 nm. G = Golgi apparatus; MN = myelinated neuron.

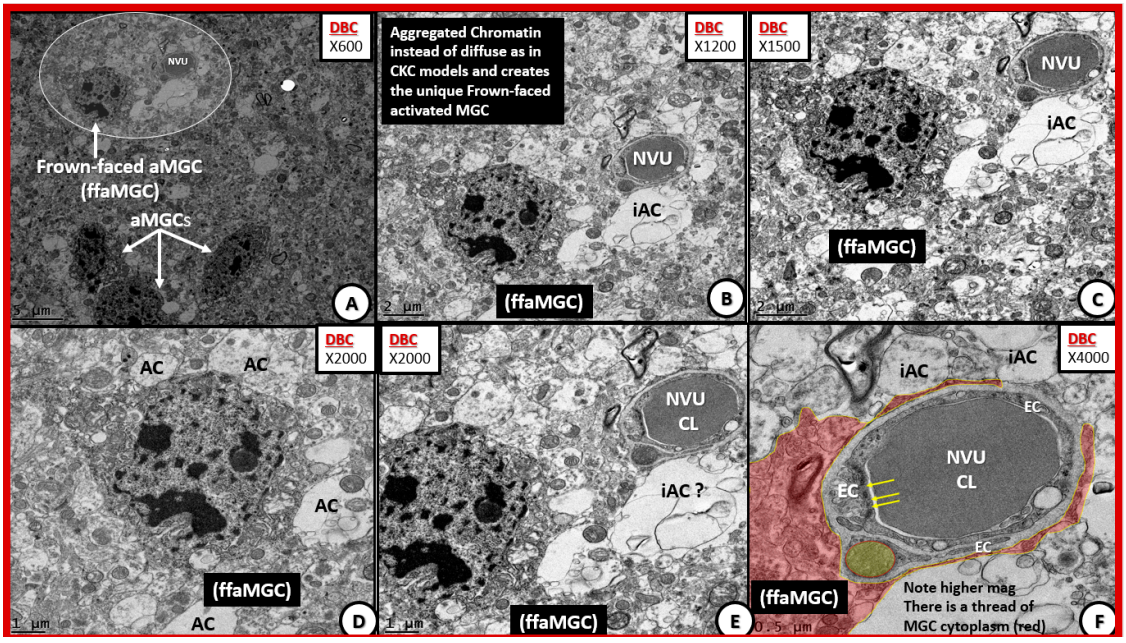

Figure 12. Activated microglia cells are associated with chromatin condensation and invasiveness of the neurovascular unit in the diabetic DBC Models. Panels (**A**–**F**) depict an activated 'frown-faced' activated/amoeboid microglia cell (aMGC) and follows it through progressively increased magnifications to demonstrate how the aMGC invades the NVU and associates with early astrocyte (AC) detachment. Additionally, note how the blood brain barrier (BBB) tight and adherent junctions (TJ/AJ) are attenuated via interruption of the normally continuous TJ/AJ of the BBB in panel (**F**). Also note in panel (**F**) that the aMGC of the 'frown-faced' microglia with marked chromatin condensation appears to not only invade but may also lift and promote the early separation of the intact AC from the basement membrane of the NVU inferiorly and superiorly. CL: capillary lumen.

The observation of aMt in aMGCs may set the stage for redox injuries not only to the microglia itself and their organelles but also the surrounding cells of the NVU.

In summary, aMGCs in the diabetic DBC may be characterized by four ultrastructure remodeling core signature changes: (i) Loss of ramified cytoplasmic extensions with amoeboid phenotypes; (ii) invasive phenotypes of the NVU; (iii) aberrant mitochondria with swelling, loss of electron-dense matrix, and loss or fragmented crista; (iv) nuclear chromatin condensation when compared to nondiabetic CKC models.

We have included the newer technology of Focused Ion Beam/Scanning Electron Microscopy (FIB/SEM) videos of the aMGC in the DBC models, which demonstrate not only the nuclear chromatin condensation but also help to better understand the 3D motion of the aM) as they come into and out of view within the cytoplasm of the DBC aMGC (Figure S4 and Video S3).

3.3. Aberrant Mitochondria in the Diabetic DBC Models

Mitochondria play a vital and essential role in nutrient metabolism of brain cells including the vascular mural cells, glia, dendritic synapses and neurons [13,15–17]. Aberrant mitochondria were primarily found to be observed in the cytoplasm of aMGCs; however, these similar aMt remodeling changes also were found in some EC, pericyte (Pc) and Pc foot processes, AC, myelinated and unmyelinated neurons within the neuropil (Figure 13).

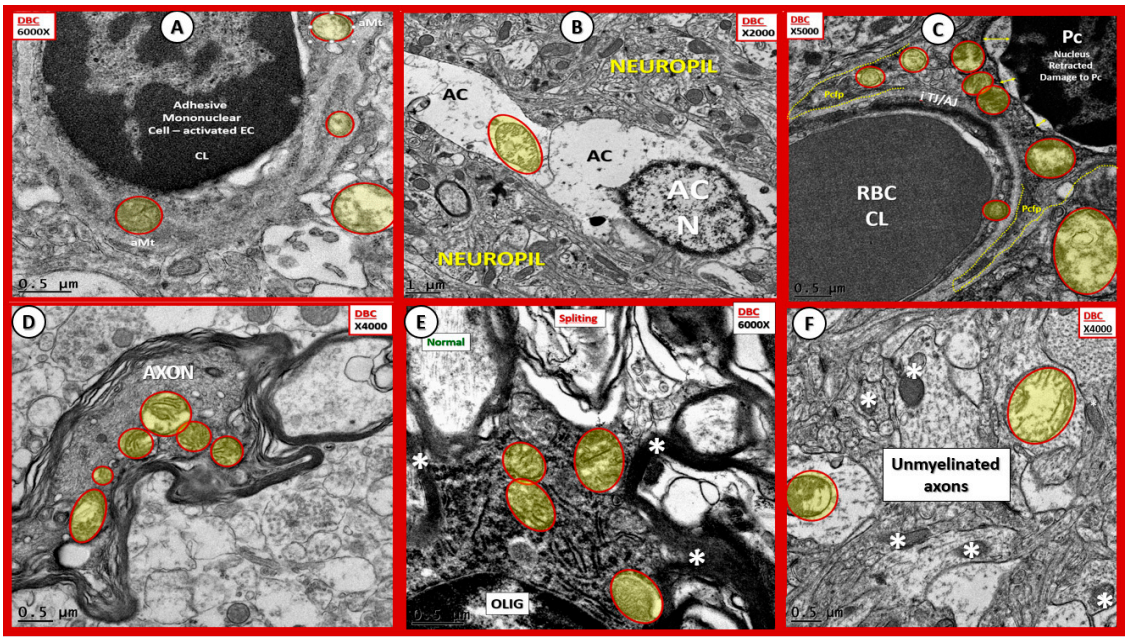

Figure 13. Aberrant mitochondria in endothelial cells, pericytes and foot processes, astrocytes, oligodendrocytes, myelinated and unmyelinated neurons. Panels (**A**–**F**) demonstrate that aberrant mitochondria (aMt) are found to be present in multiple cells in addition to activated microglia cells (aMGCs). The aMt are pseudo-colored in each of these panels (yellow outlined in red lines) in order to allow rapid recognition. Panels (**B**,**F**) are especially important since they demonstrate the aMt characterized by swollen mitochondria (Mt), loss of electron-dense Mt matrix and crista. Panel (**A**) illustrates the aMt within the endothelial cells and surrounding aMGC. Panel (**B**) depicts aMt in ACs. Panel (**C**) demonstrates aMt in pericytes and foot processes (Pc and Pcfp). Panel (**D**) depicts aMt in a dysmyelinated neuronal axon. Panel (**E**) depicts aMt in an oligodendrocyte and Panel (**F**) illustrates aMt in an AC to the left and an unmyelinated axon on the right within the neuropil. Magnifications are noted in the upper part of each panel and scale bars are located at the lower left-hand side of all panels. Scale bars = 0.5 µm in all images except for panel (**B**) with scale bar = 1 µm.

3.4. Implications of White Blood Cell (Mononuclear) Lymphocyte Adherence in DBC Models

Adherence of the mononuclear white blood cell (WBC) (lymphocyte) in some NUVs of the diabetic DBC models have allowed not only the concept of an activated endothelium in DBC to be strongly considered as compared to CKC but also have stimulated the question as to the possibility that the aMGC may also be playing a role in signaling the WBC to come in contact with the EC and adhere to an activated endothelium (Figure 13).

Previously, we had to include images of WBC adherence in Part I because there is such widespread multicellular remodeling that it is difficult to just examine one aspect of cellular remodeling in one image without including other cellular remodeling changes that concurrently occur in DBC models [1]. Also, these glial remodeling changes are associated with hyperglycemia and it is important to understand how hyperglycemia may drive the chronic neuroinflammation and the associated compromise of BBB TJ/AJ, which promote an increase in permeability and leads to memory loss and impaired cognition in T2DM mouse models in the diabetic DBC [18]. Activated microglia are known not only to contain certain cell surface receptors but also are responsible for the secretion of a specialized group of signaling cytokines and chemokines, which include monocyte chemoattractant protein 1 (MCP-1) chemokine also known as CCL2. Monocyte chemoattractant protein and other inflammatory signaling molecules are thought to signal peripheral monocytes, neutrophils and lymphocytes to adhere to the NVU endothelial cell and eventually undergo chemotaxis into the brain and migrate to regions of injury (Figure 14) [19].

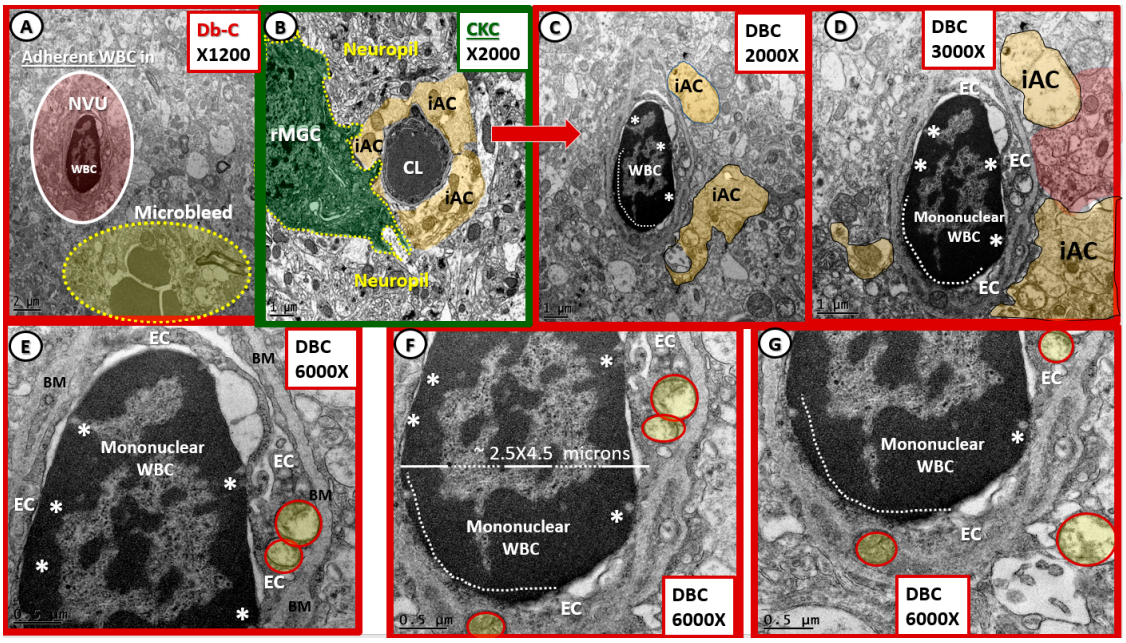

Figure 14. Compilation of white blood cell adherence in diabetic DBC models. Panels (**A**,**C**–**G**) depict multiple increasing magnifications of a white blood cell (WBC) adhering to the luminal activated endothelial cell (EC). Panel B demonstrates a surveilling ramified microglia (rMGC) and note how it is only surveilling the NVU for danger or damage signals. Also note the intact golden halo of astrocyte end feet surrounding the NVU. This is in contrast to the reactive-activated (aMGC), which appears to be invading the NVU. Note that in higher magnified images in panels (**E**–**G**) that the ECs also have aberrant mitochondria (depicted as yellow cores with encircling red lines). Also, note in (**C**,**D**) that there are some remaining intact astrocytes (iAC) to the right of the NVU (pseudo-colored golden); however to the left, note the absence of iACs adjacent to the outer basement membrane (BM) of the EC and pericyte of the NVU. Panel A depicts not only the adherence of a WBC to the activated EC but also depicts a region of microbleeds (encircled pseudo-colored yellow with yellow dashed line and the abnormal NVU with adherent WBC enclosed in a white line oval with pseudo-colored red interior. Panels (**C**–**G**) depict adhesion sites (asterisks) with a dashed line where the adherence appears to be continuous. The adherent mononuclear WBC cell is too small (2.5 × 4.5 µm) to be a monocyte and because of the thinned nearly absent cytoplasm is morphologically considered to represent a lymphocyte. Varying magnifications are present in the identifying boxes and the scale bars are present in the lower left of each image. 2;1;1;1 µm (panels (**A**–**D**) respectively) and 0.5 µm (panels (**E**,**G**) respectively).

4. Discussion

Previously, we have presented the data supporting concurrent multicellular maladaptive remodeling in the cells comprising the NVU structures I [1]. In the present paper we describe ultrastructural remodeling of activated microglia, which also contain aberrant mitochondria and NVU adherent WBCs to the activated luminal endothelial cell of the diabetic. Previously, we have posited that activated microglia may be related to accelerated aging and the increased risk of developing age-related neurodegeneration associated with T2DM (1). Furthermore, the ultrastructural changes noted in the DBC models may possibly contribute to the increased risk of developing age-related neurodegenerative disease and dementia such as sporadic Alzheimer's disease (AD) and Parkinson's disease (PD) [1].

Mitochondrial dynamics are of critical importance in T2DM [20] and it has previously been documented that there is an increase in dynamin-1-like protein (Drp1) fission protein and increased activity of the glycogen synthase kinase 3 beta (GSK3β) proteins, while fusion proteins mitofusin-2 (Mfn2) and optic atrophy 1 (OPA-1) remain similar in T2DM as healthy controls [21,22]. Subsequently,

the aberrant mitochondria are locked into a state of fission/fusion imbalance with mitochondrial fission being predominate. Further, these aberrant mitochondria may result in damage not only to the inner membranes but also the outer mitochondrial membranes that may allow for herniation and loss of the mitochondrial matrix proteins and sometimes result in mitochondria swelling (Figure 15) [23].

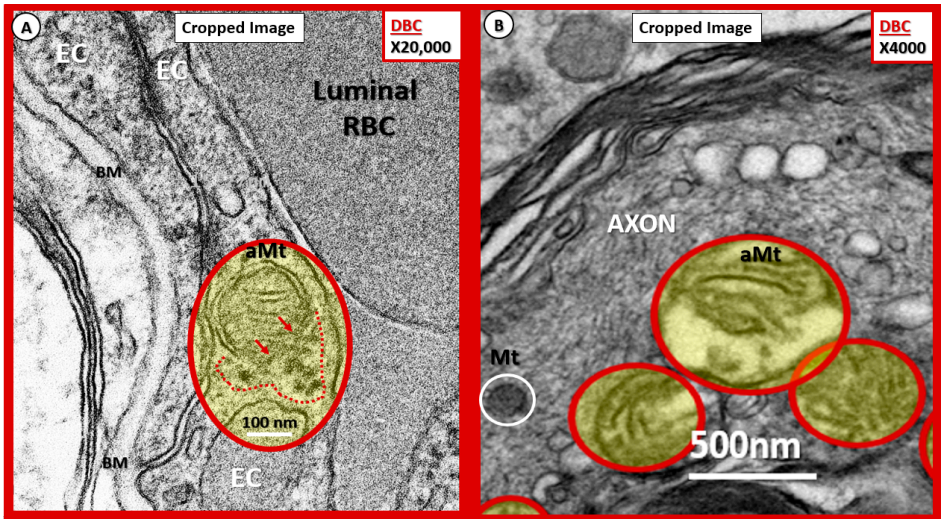

Figure 15. Possible mechanisms for the development of aberrant mitochondria (aMt) in the diabetic DBC models. (**A**,**B**) Illustrate possible Mt herniation with loss of Mt matrix proteins and crista with intact scale bars. Panel (**A**) original magnification ×20,000 with intact scale bar = 100 nm. Panel (**B**) original magnification ×4000 with intact scale bar = 500 nm. (**A**) depicts the loss of Mt matrix proteins and crista with protein aggregation into the surrounding EC cytoplasm in the aMt possibly via herniation (pseudo-colored yellow with encircling red line). Note that the outer Mt and inner Mt membranes appear to be disrupted allowing it contents to herniate outward or leak into the surrounding EC cytoplasm (arrows and red dashed lines). Interestingly, note the interruption of tight junction/adherens junction (TJ/AJ electron-dense staining where there are overlapping ECs in (**A**). Panel (**B**) also demonstrates three aMt with the superior aMt demonstrating possible herniation in a dysmyelinated neuronal axon (pseudo-colored yellow with encircling red line). Importantly, note the adjacent normal electron-dense Mt (encircled white) with electron-dense matrix and smaller size as compared to the aMt in this myelinated axon. aMt: Aberrant mitochondria; BM: Basement membrane; EC: endothelial cell; Mt: mitochondria; RBC: red blood cell.

Recently, there has been an interest in hyperglycemia-driven neuroinflammation, which may compromise the integrity of BBB with increased permeability that leads to memory loss and impaired cognition [18]. This, along with the increasing interest in the vascular contributions to cognitive impairment and dementia, wherein scientific experts convened to discuss the research gaps in our understanding of how vascular factors contribute to Alzheimer's disease and related dementia has been discussed. [24,25]. These contributions to cognitive impairment and dementia could be considered inclusive of our current findings of the NVU remodeling including the glia ultrastructural remodeling in the diabetic DBC models. We propose that this terminology would be even more inclusive and put forth the title of microvascular contributions to cognitive impairment and dementia (Figure 16). The clinical importance of which, may be discussed over the coming years and could possibly remain a constant when discussing the microvascular and glia remodeling of the brain as an end-organ in T2DM and diabetic cognopathy. The process of neuroinflammation including the activated microglia remodeling abnormalities in the DBC are also now candidates to be included in this microvascular contribution to cognitive impairment and dementia scenario. Importantly, a recent publication regarding the virtual kaleidoscopic presentation of identifying core gene microglial phenotypes and

disease-specific microglial signatures has been shared, which aid in our trek into the future along with the concept of metabolic shifts and reprogramming of microglia [12,26].

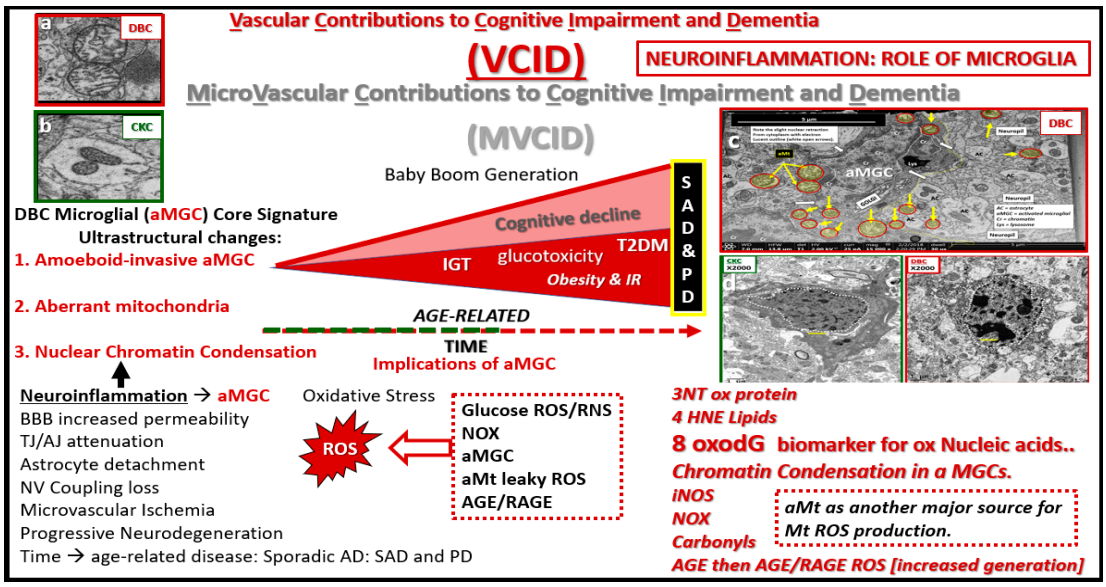

Figure 16. Microvascular contribution to cognitive impairment and dementia. This cartoon image with transmission electron microscopic image inserts (**a**–**d**) depict impaired glucose tolerance (IGT), obesity and insulin resistance (IR) in diet-induced obesity (DIO) as the disease process progresses to increased glucotoxicity to overt type 2 diabetes mellitus (T2DM) in humans and our DBC models and may be associated with increasing cognitive impairment and dementia. As previously discussed, this is associated with a plethora of morphological ultrastructural multicellular remodeling changes and abnormalities, which include activated-amoeboid microglia cells (aMGC) (insert **c**) that may be associated with increased synthesis and secretion of functional toxic cytokines and chemokines in the DBC models. These abnormalities may contribute to neurodegeneration in addition to aMGC nuclear chromatin condensation (insert **d**) and leaky aberrant Mt (aMt) (insert **a**). These aMGCs may be associated and contribute to neuroinflammation, which may lead to the development of microvascular contributions to cognitive impairment and dementia (MVCID) and furthermore, may contribute to the development of sporadic Alzheimer's disease (SAD) and sporadic Parkinson's disease (PD). AGE = advanced glycation end products; BBB: Blood brain barrier; DIO: Diet-induced obesity; Inos: Inducible nitric oxide synthase; NOX = NADPH Ox (reduced nicotinamide adenine dinucleotide phosphate); NV: Neurovascular; RAGE: Receptor for advanced glycation endproducts; ROS: Reactive oxygen species; TJ/AJ: Tight junctions/adherens junctions; 3NT: 3 nitrotyrosine; 4HNE: 4 hydroxynonenal; 8oxodG: 8-Oxo-2′-deoxyguanosine, which are biomarkers of oxidative stress for proteins, lipids, nucleic acids respectively.

Indeed, these are exciting times having identified microglial core ultrastructural phenotype signatures consisting of amoeboid phenotypes, invasive NVU phenotypes, aberrant mitochondria and chromatin condensation-compaction as described by utilizing the established technique of TEM and the newer techniques of FIB/SEM. These established and newer techniques have allowed us to further explore some of the hidden secrets as put forth in part I and now this part II series of the microglia and mitochondria.

On October 2nd, 2018, we found the following paper updating the role of microglia and feel that our readers should supplement our ultrastructural remodeling changes with a summary of the functional microglia changes put forth by Hammond T.R., Robinton D. and Stevens B. in their published preprint [27]. In the past few years there has been an explosion of functional information regarding microglia receptors and secreted proteins for surveillance and immune responses to better understand

their multiple roles. It is now very clear amongst microglia researchers that microglia may assume a myriad of activation states or spectrum changes of activation (Figure 2) from their development to their roles in forming ramified microglia to their spectrums of activated states, which includes synaptic pruning in health and disease and their supportive role of synaptic maintenance [6,27], Hammond T.R. et al. [27] state the following: "First, we must better understand the states that microglia assume in both development and disease. It is widely agreed that the term activation, or the bimodal M1/M2 scheme, does not sufficiently describe the multitude of ways in which these cells can respond to changes in their environment or the diversity of their functional states." Because of these evolving current concepts, we only discussed our observational ultrastructural remodeling changes of the microglia in relation to the neurovascular unit and other glial cells found in the female diabetic db/db models (DBC) and did not go into any depth regarding their functional changes as we were only performing ultrastructural remodeling changes. Indeed, these are exciting times to study the brain and microglial cells and reflect on the secret (the tissues [1]) to see how they undergo ultrastructural remodeling changes.

Supplementary Materials: The following are available online at http://www.mdpi.com/2571-6980/1/2/21/s1, Figure S1: Cubed image pyramidal layer III region of interest, Figure S2: Region of Interest, Figure S3: Neurovascular Unit with intact astrocytes, Figure S4: Activated microglia with aberrant mitochondria and chromatin condensation, Video S1: Microglia actively cleaning pyramidal layer III, Video S2: Ramified microglia surveilling the Neurovascular Unit, Video S3: Activated microglia with aberrant mitochondria and chromatin.

Author Contributions: M.R.H. and V.G.D. conceptualized the study; M.R.H. performed the image collection and interpretation; D.G.G. prepared the tissue specimens for transmission electron microscopic studies and assisted M.R.H.; M.R.H. prepared the manuscript; A.R.A. collected tissue specimens; V.G.D., A.R.A., and D.G.G. assisted in editing.

Funding: This study was supported by an internal grant entitled: Excellence in Electron Microscopy grant and issued by the University of Missouri Electron Microscopy Core and Office of Research. No external funding was available.

Acknowledgments: Authors wish to thank Tommi White of the University of Missouri Electron Microscopy Core Facility. Authors also wish to thank our mentor James R. Sowers, who inspired us to interrogate, characterize, and understand the secrets that the tissues behold.

Conflicts of Interest: The authors declare no conflicts of interest.

References

1. Hayden, M.R.; Grant, D.; Aroor, A.; Demarco, V.G. Ultrastructural remodeling of the neurovascular unit in the female diabetic db/db Model—Part I: Astrocyte. *Neuroglia* **2018**, *1*, 15. [CrossRef]
2. Tambuyzer, B.R.; Ponsaerts, P.; Nouwen, E.J. Microglia: Gatekeepers of the central nervous system immunology. *J. Leukoc. Biol.* **2009**, *85*, 352–370. [CrossRef] [PubMed]
3. Pósfai, B.; Cserép, C.; Orsolits, B.; Dénes, Á. New Insights into microglia-neuron interactions: A neuron's perspective. *Neuroscience* **2018**. [CrossRef] [PubMed]
4. Liu, Y.; Li, M.; Zhang, Z.; Ye, Y.; Zhou, J. Role of microglia-neuron interactions in diabetic encephalopathy. *Ageing Res. Rev.* **2017**, *42*, 28–39. [CrossRef] [PubMed]
5. Glass, C.K.; Saijo, K.; Winner, B.; Marchetto, M.C.; Gage, F.H. Mechanisms underlying inflammation in neurodegeneration. *Cell* **2010**, *140*, 918–934. [CrossRef] [PubMed]
6. Koellhoffer, E.C.; McCullough, L.D.; Ritzel, R.M. Old maids: Aging and its impact on microglia function. *Int. J. Mol. Sci.* **2017**, *18*, 769. [CrossRef] [PubMed]
7. Tang, Y. Editorial: microglial polarization in the pathogenesis and therapeutics of neurodegenerative diseases. *Front. Aging Neurosci.* **2018**, *10*, 154. [CrossRef] [PubMed]
8. Tang, Y.; Le, W. Differential roles of M1 and M2 microglia in neurodegenerative diseases. *Mol. Neurobiol.* **2016**, *53*, 1181–1194. [CrossRef] [PubMed]
9. Crotti, A.; Ransohoff, R.M. Microglial physiology and pathophysiology: Insights from genome-wide transcriptional profiling. *Immunity* **2016**, *44*, 505–515. [CrossRef] [PubMed]
10. Ransohoff, R.M.; Perry, V.H. Microglial physiology: Unique stimuli, specialized responses. *Annu. Rev. Immunol.* **2009**, *27*, 119–145. [CrossRef] [PubMed]

11. Ransohoff, R.M. A polarizing question: Do M1 and M2 microglia exist? *Nat. Neurosci.* **2016**, *19*, 987–991. [CrossRef] [PubMed]
12. Orihuela, R.; McPherson, C.A.; Harry, G.J. Microglial M1/M2 polarization and metabolic states. *Br. J. Pharmacol.* **2016**, *173*, 649–665. [CrossRef] [PubMed]
13. Sousa, C.; Biber, K.; Michelucci, A. Cellular and molecular characterization of microglia: A unique immune cell population. *Front. Immunol.* **2017**, *8*, 198. [CrossRef] [PubMed]
14. Hayden, M.R.; Banks, W.A.; Shah, G.N.; Gu, Z.; Sowers, J.R. Cardiorenal metabolic syndrome and diabetic cognopathy. *Cardiorenal Med.* **2013**, *3*, 265–282. [CrossRef] [PubMed]
15. Abdul-Ghani, M.A.; DeFronzo, R.A. Mitochondrial dysfunction, insulin resistance, and type 2 diabetes mellitus. *Curr. Diabetes Rep.* **2008**, *8*, 173–178. [CrossRef]
16. Yu, L.; Fink, B.D.; Herlein, J.A.; Sivitz, W.I. Mitochondrial function in diabetes: Novel methodology and new insight. *Diabetes* **2013**, *62*, 1833–1842. [CrossRef] [PubMed]
17. Sivitz, W.I.; Yorek, M.A. Mitochondrial dysfunction in diabetes: From molecular mechanisms to functional significance and therapeutic opportunities. *Antioxid. Redox Signal.* **2010**, *12*, 537–577. [CrossRef] [PubMed]
18. Rom, S.; Zuluaga-Ramirez, V.; Gajghate, S.; Seliga, A.; Winfield, M.; Heldt, N.A.; Kolpakov, M.A.; Bashkirova, Y.V.; Sabri, A.K.; Persidsky, Y. Hyperglycemia-driven neuroinflammation compromises BBB leading to memory loss in both diabetes mellitus (DM) type 1 and type 2 mouse models. *Mol. Neurobiol.* **2018**, 1–14. [CrossRef] [PubMed]
19. Deshmane, S.L.; Kremlev, S.; Amini, S.; Sawaya, B.E. Monocyte chemoattractant protein-1 (MCP-1): An overview. *J. Interferon Cytokine Res.* **2009**, *29*, 313–326. [CrossRef] [PubMed]
20. Rovira-Llopis, S.; Bañuls, C.; Diaz-Morales, N.; Hernandez-Mijares, A.; Rocha, M.; Victor, V.M. Mitochondrial dynamics in type 2 diabetes: Pathophysiological implications. *Redox Biol.* **2017**, *11*, 637–645. [CrossRef] [PubMed]
21. Huang, S.; Wang, Y.; Gan, X.; Fang, D.; Zhong, C.; Wu, L.; Hu, G.; Sosunov, A.A.; McKhann, G.M.; Yu, H.; et al. Drp1-mediated mitochondrial abnormalities link to synaptic injury in diabetes model. *Diabetes* **2015**, *64*, 1728–1742. [CrossRef] [PubMed]
22. Gottlieb, R.A.; Daniel Bernstein, D. Mitochondrial remodeling: Rearranging, recycling, and reprogramming. *Cell Calcium* **2016**, *60*, 88–101. [CrossRef] [PubMed]
23. Sesso, A.; Belizário, J.E.; Marques, M.M.; Higuchi, M.L.; Schumacher, R.I.; Colquhoun, A.; Ito, E.; Kawakami, J. Mitochondrial swelling and incipient outer membrane rupture in preapoptotic and apoptotic cells. *Anat. Rec. (Hoboken)* **2012**, *295*, 1647–1659. [CrossRef] [PubMed]
24. Snyder, H.M.; Corriveau, R.A.; Craft, S.; Faber, J.E.; Greenberg, S.M.; Knopman, D.; Lamb, B.T.; Montine, T.J.; Nedergaard, M.; Schaffer, C.B.; et al. Vascular contributions to cognitive impairment and dementia including Alzheimer's disease. *Alzheimer's Dement.* **2015**, *11*, 710–717. [CrossRef] [PubMed]
25. Corriveau, R.A.; Bosetti, F.; Emr, M.; Gladman, J.T.; Koenig, J.I.; Moy, C.S.; Pahigiannis, K.; Waddy, S.P.; Koroshetz, W. the science of vascular contributions to cognitive impairment and dementia (VCID): A framework for advancing research priorities in the cerebrovascular biology of cognitive decline. *Cell Mol. Neurobiol.* **2016**, *36*, 281–288. [CrossRef] [PubMed]
26. Dubbelaar, M.L.; Kracht, L.; Eggen, B.J.L.; Boddeke, E. The kaleidoscope of microglial phenotypes. *Front. Immunol.* **2018**. [CrossRef] [PubMed]
27. Hammond, T.R.; Robinton, D.; Stevens, B. Microglia and the brain: complementary partners in development and disease. *Annu. Rev. Cell Dev. Biol.* **2018**, 34. [CrossRef] [PubMed]